

Mapping Soil Electrical Conductivity Using Ordinary Kriging Combined with Back-propagation Network

HUANG Yajie¹, LI Zhen¹, YE Huichun², ZHANG Shiwen^{1,3}, ZHUO Zhiqing¹, XING An¹, HUANG Yuanfang¹

(1. Key Laboratory of Arable Land Conservation (North China), Ministry of Agriculture/Key Laboratory of Agricultural Land Quality Monitoring, Ministry of Land and Resources, College of Resources and Environmental Sciences, China Agricultural University, Beijing 100193, China; 2. Key Laboratory of Digital Earth Science, Institute of Remote Sensing and Digital Earth, Chinese Academy of Sciences, Beijing 100094, China; 3. School of Earth and Environment, Anhui University of Science and Technology, Huainan 232001, China)

Abstract: Accurate mapping of soil salinity and recognition of its influencing factors are essential for sustainable crop production and soil health. Although the influencing factors have been used to improve the mapping accuracy of soil salinity, few studies have considered both aspects of spatial variation caused by the influencing factors and spatial autocorrelations for mapping. The objective of this study was to demonstrate that the ordinary kriging combined with back-propagation network (OK_BP), considering the two aspects of spatial variation, which can benefit the improvement of the mapping accuracy of soil salinity. To test the effectiveness of this approach, 70 sites were sampled at two depths (0–30 and 30–50 cm) in Ningxia Hui Autonomous Region, China. Ordinary kriging (OK), back-propagation network (BP) and regression kriging (RK) were used in comparison analysis; the root mean square error (*RMSE*), relative improvement (*RI*) and the decrease in estimation imprecision (*DIP*) were used to judge the mapping quality. Results showed that OK_BP avoided the both underestimation and overestimation of the higher and lower values of interpolation surfaces. OK_BP revealed more details of the spatial variation responding to influencing factors, and provided more flexibility for incorporating various correlated factors in the mapping. Moreover, OK_BP obtained better results with respect to the reference methods (i.e., OK, BP, and RK) in terms of the lowest *RMSE*, the highest *RI* and *DIP*. Thus, it is concluded that OK_BP is an effective method for mapping soil salinity with a high accuracy.

Keywords: ordinary kriging; neural network; soil electrical conductivity; variability; mapping; Ningxia, China

Citation: HUANG Yajie, LI Zhen, YE Huichun, ZHANG Shiwen, ZHUO Zhiqing, XING An, HUANG Yuanfang, 2019. Mapping Soil Electrical Conductivity Using Ordinary Kriging Combined with Back-propagation Network. *Chinese Geographical Science*, 29(2): 270–282. https://doi.org/10.1007/s11769-019-1027-1

1 Introduction

Soil salinity is a severe environmental factor limiting soil fertility in agricultural lands. It can damage sustainable crop production and soil health. The production of agricultural crops is difficult in saline and sodic soils, which has attracted great concern from farmers, government and environmental scientists (Bilgili et al.,

2013; Chen et al., 2014; Zhao et al., 2016). Accurate mapping of the soil salinity and recognition of its influencing factors are necessary for crop production and sustainable soil utilization (Ding and Yu, 2014; Taghizadeh-Mehrjardi et al., 2016).

Soil salinity is the combined effect of natural and anthropogenic processes. The natural factors influencing the spatial distribution of soil salinity include soil types

Received date: 2017-11-29; accepted date: 2018-03-14

Foundation item: Under the auspices of the National Natural Science Foundation of China (No. 41571217), the National Key Research and Development Program of China (No. 2016YFD0300801)

Corresponding author: HUANG Yuanfang. E-mail: yfhuang@cau.edu.cn

© Science Press, Northeast Institute of Geography and Agroecology, CAS and Springer-Verlag GmbH Germany, part of Springer Nature 2019

(Fang et al., 2005; Yu et al., 2014), soil water content (Wu et al., 2014), geology (Sheng et al., 2010; Yu et al., 2014), climate (Nosetto et al., 2008), normalized difference vegetation index (NDVI) (Yahiaoui et al., 2015) and soil texture (Wang et al., 2012; Zhao et al., 2016). The anthropogenic factors include irrigation practices (Akramkhanov et al., 2011), drainage systems (Mirlas et al., 2012; Yu et al., 2015), groundwater table (Shah et al., 2011; Wu et al., 2014) and land use (Akramkhanov et al., 2011; Nosetto et al., 2013). It is widely established that using correlated influencing factors as auxiliary variables can improve the mapping accuracy of soil properties (Liu et al., 2006; Zhang et al., 2013).

Numerous methods have been developed to map the spatial distribution of soil properties. These methods can be classified into three categories: geostatistical methods, such as ordinary kriging (OK) (Mueller et al., 2004; Ye et al., 2016); hybrid models, such as regression kriging (RK) (Hengl et al., 2004; Ye et al., 2017); simple statistical methods, such as multiple linear regression (MLR) (Mora-Vallejo et al., 2008; Yang et al., 2014), artificial neural networks (Sarangi et al., 2006; Huang et al., 2017) and random forest (Were et al., 2015; Raczko and Zagajewski, 2017).

Ordinary kriging (OK) is one of the most basic geostatistical types, however, it does not consider the environment factors. Soil salinity variations do not always satisfy the stationary assumptions of kriging methods due to its complex variations. In addition, the environment factors at different local positions in the study area have different influences on the soil properties. The relationships between soil properties and environmental factors are rarely linear in nature, and vary in each region (Zhao et al., 2010; Shahabi et al., 2017). Therefore, the hybrid models, such as RK, simply based on the same regression equation to explore the linear relationships between soil properties and environmental factors in the whole study region, lead to the prediction imprecision (McBratney et al., 2003; Li et al., 2016). Accordingly, these methods are limited to model soil salinity variations.

With respect to the simple statistical methods, artificial neural networks (ANNs) reveals much greater spatial details and has better soil mapping (Zhu et al., 2000; Akramkhanov and Vlek, 2012; Dai et al., 2014; Huang et al., 2015). Firstly, the relationships between soil properties and environmental variables are assumed linear by linear regression. Actually, the relationships are

not always linear for all locations in an entire area (Lark, 1999). Secondly, although both ANNs and random forest are applied to explore the nonlinear and complicated relationships, the former ANNs presents higher quality and better performance than random forest in prediction and classification (Were et al., 2015; Raczko and Zagajewski, 2017). Thirdly, ANNs is one of the most commonly used approaches in salinity studies, including soil salinity prediction of crop root zone (Patel et al., 2002), saturated hydraulic conductivity (Motaghian and Mohammadi, 2011; Sedaghat et al., 2016) and soil salinity mapping (Zou et al., 2010; He et al., 2015). Nevertheless, ANNs only consider the variations of the soil properties caused by the correlated environmental factors or the spatial autocorrelation of surrounding measured data (Park and Vlek, 2002; Takata et al., 2007). The use of ANNs combined with both the spatial auto-correlative information and the environmental factors into mapping, however, has little been reported to date.

The objective of this study is to examine whether the OK_BP can improve the mapping accuracy. Back-propagation network (BP) is used to explain the spatial variability caused by the selected influencing factors, and OK is used to explore the spatial autocorrelation in BP prediction residuals. OK, BP and RK are compared in order to verify the effectiveness of OK_BP. The mean absolute error (*MAE*), root mean squared errors (*RMSE*), the relative improvement (*RI*) and the decrease in estimation imprecision (*DIP*) are used to evaluate the performances of the different methods.

2 Materials and Methods

2.1 Study area

The study is conducted in the Xidatan region (38°47'58"N–38°49'47"N, 106°24'48"E–106°26'10"E), which is situated in Pingluo County, Ningxia Hui Autonomous Region, Northwest China (Fig. 1). The study area is in a field of about 354 ha with arable land and low-lying abandoned land. A large area of highly saline-sodic soil exists in the field. Developed in alluvial deposits, the soil is classified as takyric solonetz (IUSS Working Group WRB, 2007). The soil salinization affects the sustainability of agricultural production in this area, where the groundwater level is closer to the surface accompanied with poor drainage and semi-arid climate. The evaporation rate is high (875 mm/yr) compared to precipitation (205 mm/yr). In

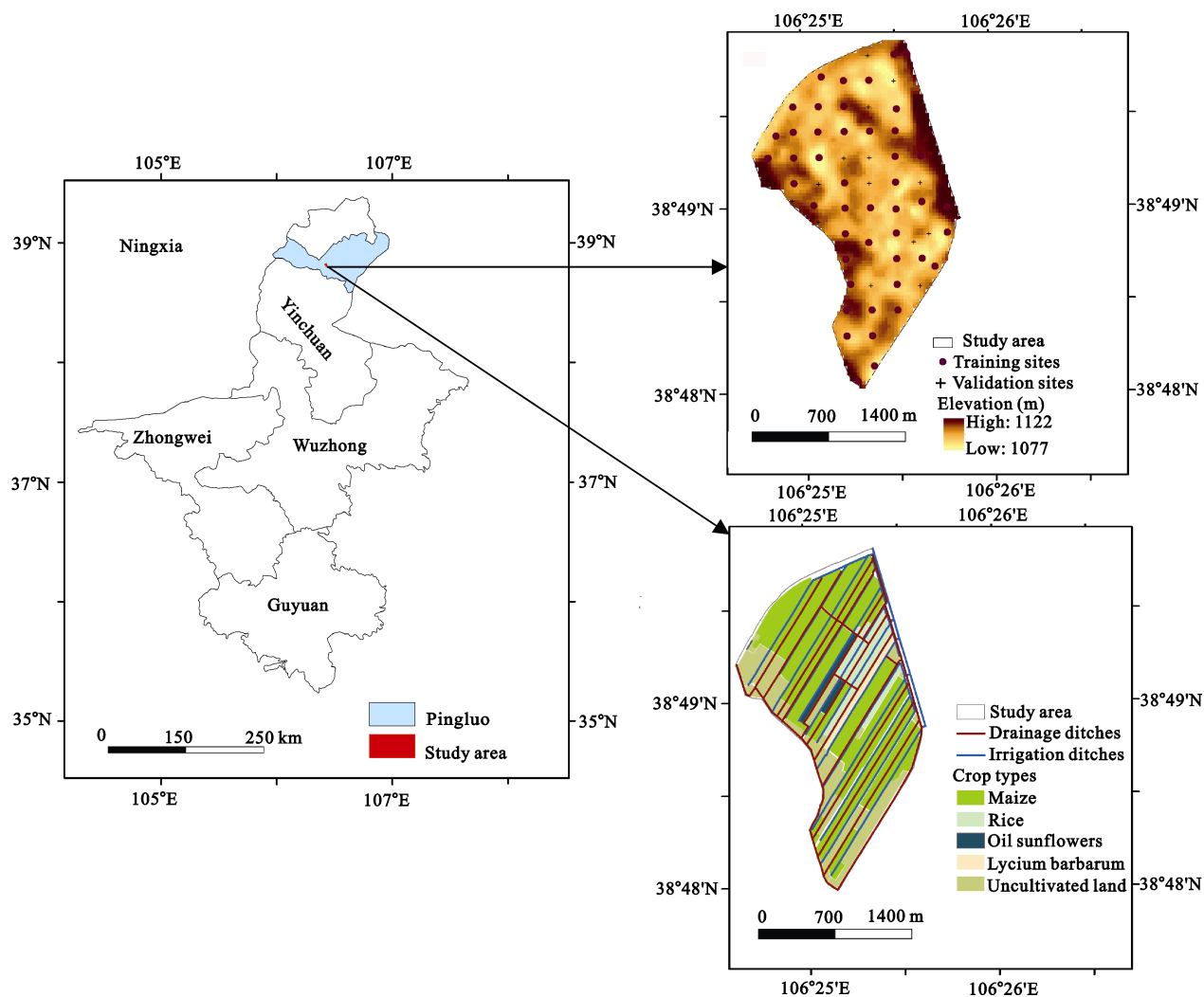


Fig. 1 Location of the study area, the spatial distribution of soil samples and crop types

addition, the disorderly reclamation of farmland and extensive anthropogenic management contribute to increasing the soil salinization. The soil salinity exhibits high spatial heterogeneity.

2.2 Data and processing

A 240 m grid sampling strategy was used to characterize saline-sodic soils, which was implemented by the fish-net tool of ArcGIS 10.0 (ESRI, Inc., Redlands, CA, USA). 70 locations were sampled at two different depths (0–30 and 30–50 cm). A 10 fold cross validation approach was adopted to validate the accuracy of the algorithms (Mirakzehi et al., 2018; Wang et al., 2018). Soil samples were collected at May, 2016. Each composite soil sample comprised four core subsamples that were collected at a distance of 5 m north, south, east and west

of the center sampling points.

The soil samples were crushed and mixed together to form one sample. Soil samples were dried, and ground to pass through a 2-mm sieve. Next, the ground and sieved soil samples were mixed with water at a 1 (soil sample): 5 (water) ratio at a temperature of 25°C. The leaking liquid was extracted to measure the soil electrical conductivity as detailed in the Analysis Methods of Soil Agricultural Chemistry (Lu et al., 2000). 1 (soil sample): 5 (water) soil electrical conductivity and soil salinity are usually highly correlated, and the former is often used as a surrogate for the latter (Visconti et al., 2010; Zhang et al., 2009). This was indeed the case in this study, where the soil electrical conductivity and salinity measured from the samples were highly correlated (coefficients of determination R^2 are 0.889 at 0–30 cm depth and 0.929 at 30–50 cm

depth). Accordingly, soil electrical conductivity was used to represent soil salinity.

Soil types, climate, soil texture are relatively unitary since the study scale is small. It is obvious that groundwater table and irrigation practices remain nearly consistent when sampling in study area, and therefore they cannot reflect the influence on spatial variability of soil salinity. Then, we select elevation, NDVI, land use types, drainage and irrigation as environmental factors for mapping soil electrical conductivity. The effectiveness of these factors on soil electrical conductivity will be further investigated by sensitivity analysis. The 30 m resolution Digital Elevation Model (DEM) was derived from a 1:10 000 scale topographic map provided by Chinese Bureau of Surveying. To ensure that NDVI can adequately indicate soil salinity, we downloaded it at July 17, 2016, without clouds. The NDVI at 30 m spatial resolution was derived from a Landsat 8 image (<http://ids.ceode.ac.cn/index.aspx>), and it had an obvious connection with the soil salinity. According to the field survey, the predominant crop type was maize. The rice, oil sunflowers and lycium barbarum were dispersedly distributed in study area. The irrigation and drainage were calculated by the shortest distances from the centers of fields to the irrigation ditches (or drainage ditches), which were implemented by analysis tool available in ArcGIS 10.0.

2.3 Methods

2.3.1 Ordinary kriging combined with back-propagation network (OK_BP)

BP as a simple structure of ANNs is used to simulate the nonlinear complex system. The BP normally includes three layers: input layer, hidden layer and output layer. Each layer is composed of neurons and fully connected to the preceding layer by interconnection weights (w_i). At the input layers, when an input neuron receives a signal (x_i), it is transmitted to the hidden layers as z_j . At the hidden layers, each neuron computes the sum $w_{il}z_j$ and then applies a nonlinear activation function f_2 to produce an output signal z_{il} . The process can be expressed as:

$$z_j = f_1 \left(\sum_{i=1}^5 w_{ij}x_i - b_j \right) \quad (1)$$

$$z_{il} = f_2 \left(\sum_{j=1}^l w_{il}z_j - b_l \right) \quad (2)$$

where, x_i is the input vector. In this study, the input vectors include the elevation (x_1), land use (x_2), NDVI (x_3), distance to the drainage ditches (x_4), and distance to the irrigation ditches (x_5). z_{il} as an output vector represents the soil electrical conductivity. w_{ij} is the interconnection weight between the input layer and hidden layer, while w_{il} is the interconnection weight between the hidden layer and output layer. b_j is the bias parameter between the input layer and hidden layer, while b_l is the bias parameter between the hidden layer and output layer. i , l and j denote the number of input, hidden and output nodes, respectively. In general, the optimal number of hidden nodes can be defined as:

$$l < \sqrt{(i + j)} + a \quad (3)$$

where, a is the constant with the range of 0–10. The network is trained by a back-propagation algorithm and conjugate gradient learning algorithms, which adjusts the weights and biases to minimize the error. The error is calculated using the following equation:

$$EP = \frac{\sum_{i=1}^m (z_{il} - z_i)^2}{2} \quad (4)$$

where, EP is the error value. z_i represents the measured values of soil electrical conductivity. m is the sampling numbers.

In order to identify how the input factors exert their influence on the soil electrical conductivity, sensitivity analysis is trained by removing one input factor at a time while not changing any of another item for every pattern. The algorithm can be defined as:

$$SI_i = RMSE_i / RMSE_a \quad (5)$$

where, SI_i is the sensitive index. $RMSE_i$ and $RMSE_a$ are the root mean squared errors of the default i th input factors and all factors entering the input layer, respectively. The value of SI_i is larger, the input factor is more sensitive. The detailed algorithm is explained elsewhere (Olden and Jackson, 2002; Mozumder and Laskar, 2015). The BP procedures are carried out in MATLAB 6.1 (MathWorks, Inc., Natick, MA, USA).

The preceding BP is used to explain the nonlinear relationships between selected influencing factors and soil

electrical conductivity. OK is used to estimate residuals from BP. Then, the target variable (i.e., soil electrical conductivity) can be calculated as:

$$z(x_o) = \hat{z}_{il}(x_o) + r(x_o) \quad (6)$$

where $z(x_o)$ is the estimated value of the target variable at location x_o . $\hat{z}_{il}(x_o)$ is the predicted value by BP based on the nonlinear relationship. $r(x_o)$ is the OK prediction of the residual. The final estimated soil electrical conductivity is obtained as the sum of BP estimates $\hat{z}_{il}(x_o)$ and OK estimates of the residuals $\hat{r}_{ok}(x_o)$. It is expressed as follows:

$$\hat{z}(x_o) = \hat{z}_{il}(x_o) + \hat{r}_{ok}(x_o) \quad (7)$$

The processes are calculated using ArcGIS 10.0. The detailed steps are shown in Fig. 2. To assess the feasibility of OK_BP, other methods such as OK, BP and RK are used to evaluate their mapping performances.

2.3.2 Ordinary kriging

OK is used to estimate the residual. It depends on the fact that the closer observations are more correlated and similar. The core of geostatistics is the variogram, which expresses the spatial dependence between near observations (Isaaks and Srivastava, 1989). Detailed descriptions of OK can be found elsewhere (Eldeiry and Garcia, 2012).

2.3.3 Multiple linear regression

The multiple linear regression (MLR) aims to produce a dependent prediction between more explanatory variables and a response variable by fitting a linear equation to training sites. In this study, the environmental vari-

ables holding the strongest correlation with the predicted variable are determined as first inputs of MLR, and then the rest of the variables are examined and selected as inputs if they can increase the coefficient of determination of MLR. The detailed illustration of the computing methods can be found elsewhere (Zhang et al., 2012; Zhang et al., 2013). MLR analysis is performed using SPSS 16.0 (SPSS Inc., Chicago, IL, USA).

2.3.4 Regression kriging

RK can consider the auxiliary variables at those location points for interpolation of the outputs, which is restricted in the simple kriging method (Hengl et al., 2007). It is based on the idea that the deterministic component of the target variable is explained by a MLR model, and is then formed by summing the regression prediction and the ordinary kriging prediction of the residual at points. The process of RK can be summarized as follows:

$$Z_{RK}^*(x_o) = m^*(x_o) + r^*(x_o) \quad (8)$$

where, $Z_{RK}^*(x_o)$ represents the predicted value of the soil electrical conductivity by RK, $m^*(x_o)$ is the predicted value of soil electrical conductivity by the regression model, and $r^*(x_o)$ is residuals of the regression by semivariogram and OK.

2.4 Evaluation of mapping performance

After 10 fold cross-validation, the mean error (ME), the root mean square error (RMSE), the relative improvement (RI) and the decrease in estimation imprecision (DIP) of methods relative to OK for the validation sites are

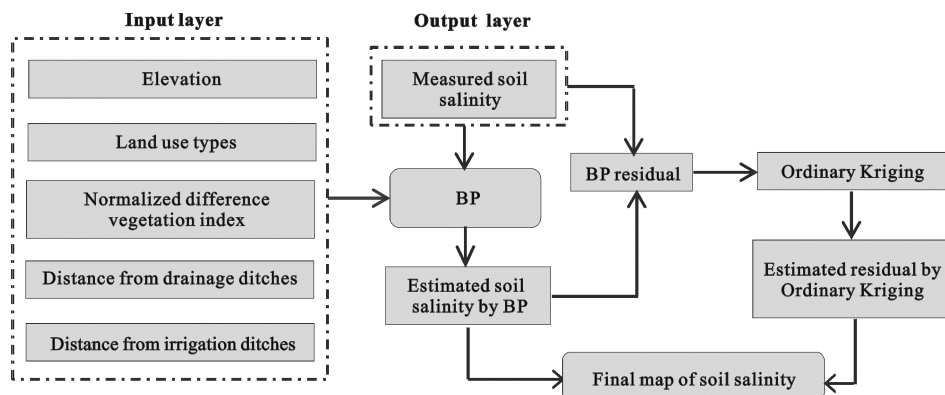


Fig. 2 Schematic illustration of the procedure to run ordinary kriging combined with back-propagation network. BP, back-propagation network.

calculated to assess the accuracy of the mapping soil electrical conductivity. Detailed descriptions of these indexes can be found elsewhere (Pang et al., 2009; Mueller and Pierce, 2003; Liu et al., 2006). *RI*, *IP* and *DIP* are expressed as follows:

$$RI = \frac{RMES_{ref} - RMSE_e}{RMES_{ref}} \times 100\% \quad (9)$$

$$IP(x_o) = RMSE^2(x_o) - ME^2(x_o) \quad (10)$$

$$DIP = \frac{\sum_{o=1}^n IP^2(x_o)_{ref} - \sum_{o=1}^n IP^2(x_o)_e}{\sum_{o=1}^n IP^2(x_o)_{ref}} \times 100\% \quad (11)$$

where, n is the number of validation points. $RMSE_{ref}$ is the root mean square error of the given reference method (OK), while $RMSE_e$ is the root mean square errors of the evaluated methods (i.e., BP, RK and OK_BP). $IP(x_o)_{ref}$ is the value of *IP* given the reference method (OK), while $IP(x_o)_e$ is the decrease imprecision (*IP*) of the evaluated methods (i.e., BP, RK and OK_BP). Positive values of *RI* and *DIP* indicate that the evaluated methods can improve the mapping accuracy of the soil electrical conductivity.

3 Results

3.1 Descriptive statistics for soil electrical conductivity

The data presented in Table 1 showed that the averages of the soil electrical conductivity for training sites at 0–30 cm and 30–50 cm were 1.03 dS/m and 0.55 dS/m, respectively. The soil electrical conductivity decreased with the increase of soil depth, which indicated that salts accumulated on the soil surface. According to the

classification standard of variability by Nielsen and Bouma (1985), the soil salinity displays strong, medium and weak variability when the coefficient of variations is < 10%, 10%–100% and > 100%, respectively. Accordingly, there were strong and medium spatial variability at the soil depths of 0–30 and 30–50 cm, respectively. The soil electrical conductivity for the training sites was positively skewed, while the log-transformed soil electrical conductivity showed approximately normal distribution. Therefore, the mapping of soil electrical conductivity was conducted by log-transformed values, and ultimately, the prediction values of the soil electrical conductivity were back-transformed into the original values using the antilogarithmic function.

3.2 Sensitivity analysis for soil electrical conductivity

Sensitivity analysis showed that the response of BP was highly dependent on the influencing factors (Table 2). It provided a measure of the relative importance among the inputs of the neural model. In this study, when each input factor was removed at a time while not changing any of another item, each *SI* showed more than 1. It revealed that all input factors exerted these influences on the soil electrical conductivity at 0–30 and 30–50 cm soil depths. According to the values of *SI*, the decreasing orders of input importance at 0–30 cm soil depth were as follows: land use types, the distance to irrigation ditches, elevation, distance to drainage ditches and NDVI. The decreasing orders of importance at 30–50 cm depth were as follows: land use types, elevation, distance to the irrigation ditches, distance to the drainage ditches and NDVI.

Table 1 Descriptive statistics of soil electrical conductivity (dS/m) at two soil depths

Layer (cm)	Data sets	Min	Max	Ave	SD	CV	Raw data		Log-transformed data		
							Skew	Kurt	Skew	Kurt	P
0–30	Training sites	0.17	5.14	1.03	1.12	1.08	1.42	0.73	0.60	0.74	0.055
	Validation sites	0.22	5.03	0.87	0.57	0.66	1.59	0.44	0.49	−0.58	0.605
30–50	Training sites	0.15	2.28	0.55	0.46	0.84	1.31	0.92	0.34	−1.02	0.319
	Validation sites	0.18	2.23	0.41	0.14	0.60	1.26	0.34	0.68	−0.06	0.606

Notes: Min, minimum; Max, maximum; Ave, average; *SD*, standard deviation; *CV*, coefficient of variation; *Skew*, skewness; *Kurt*, kurtosis.

Table 2 Validation results of sensitivity analysis by back-propagation network

Layer (cm)	Item	<i>ME</i>	<i>MAE</i>	<i>RMSE</i>	<i>SI</i>	Rank of sensitivity
0–30	All factors	–0.226	0.498	0.844	–	–
	Elevation	–0.025	0.564	0.986	1.169	3
	NDVI	0.056	0.505	0.904	1.071	5
	LU	0.168	1.123	1.656	1.962	1
	DD	0.126	0.632	0.977	1.158	4
	DI	–0.236	0.631	1.039	1.231	2
30–50	All factors	–0.180	0.302	0.572	–	–
	Elevation	0.227	0.451	0.693	1.212	2
	NDVI	0.115	0.475	0.654	1.143	5
	LU	0.001	0.614	0.835	1.460	1
	DD	0.280	0.425	0.673	1.177	4
	DI	0.195	0.434	0.681	1.191	3

Notes: NDVI, normalized difference vegetation index; LU, land use types; DD, distance to the drainage ditches; DI, distance to the irrigation ditches; *ME*, mean error; *MAE*, mean absolute error; *RMSE*, root mean squared error; *SI*, sensitive index. ‘–’ as a standard of sensitive index represents all factors entering the input layer.

3.3 Performance of BP and MLR models

BP network was trained with the input factors. In particular, it is worth noting that the optimal number of hidden neurons influenced on the mapping accuracy of the soil electrical conductivity. On the basis of the hidden nodes in Eq. (3), the number of hidden layer neurons was 1 to 12 (Fig. 3). When the number was less than 7, the prediction accuracy kept decreasing with increasing *RMSE* and *MAE*. On the other hand, BP could be over-fitted when the number of hidden layer neurons was larger than 7 (Fig. 3). Accordingly, on the basis of the minimum *MAE* and *RMSE*, the optimum structures of network were 5-7-1 at two soil depths, indicating that there were five input nodes in the input

layer, seven nodes in the hidden layer, and one node in the output layer. The best performance of BP was applied to map the soil electrical conductivity.

The soil electrical conductivity was fitted with the selected factors by the MLR model. As shown in Table 3, land use types and distance to the irrigation ditches entered into the regression equation at 0–30 cm depth, while land use types and NDVI entered into the equation at 30–50 cm depth. The relationships between soil electrical conductivity and its related influencing factors were extremely significant ($P < 0.001$), which indicated that the selected factors could explain the variability of soil electrical conductivity. Therefore, these factors were selected to predict the spatial distribution of soil electrical conductivity.

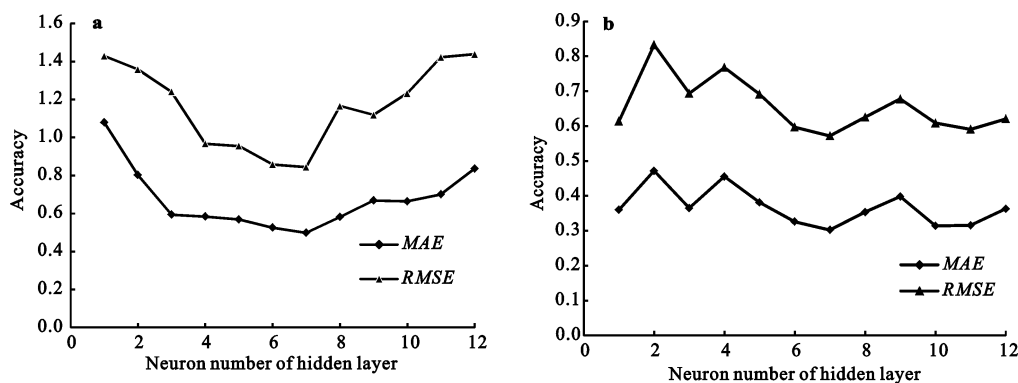


Fig. 3 Variation of the root mean squared error (*RMSE*) and mean absolute error (*MAE*) with increasing hidden neurons in the optimization of the back-propagation network (BP) model at 0–30 cm (a) and 30–50 cm (b) soil depths

Table 3 Fitted equations of multiple linear regression models for different soil depths

Layer (cm)	Fitted equations	R^2	F	P
0–30	$EC=0.295 \times LU+0.005 \times DI-0.055$	0.362	11.673	<0.001
30–50	$EC=0.157 \times LU+1.266 \times NDVI-0.224$	0.323	10.643	<0.001

Notes: EC, soil electrical conductivity; LU, land use types; DI, distance to the irrigation ditches; NDVI, normalized difference vegetation index.

3.4 Semivariogram analysis

The residuals of the soil electrical conductivity were acquired for the training sites with combinations of different variables (residuals_{RK} and residuals_{OK_BP}) (Table 4). On the basis of the Kolmogorov-Smirnov test, the raw data of the prediction residuals for OK_BP were closer to normal distribution ($P > 0.05$). By logarithmic transformation, soil electrical conductivity and residuals of RK model followed normal distribution, at 0–30 cm depth, the P -values of the soil electrical conductivity and residuals of RK model were 0.21 and 0.14; at 30–50 cm depth, the P -values are corresponded to 0.21 and 0.14. At 0–30 cm depth, the exponential model provided the best fit to the semivariogram in OK and the residuals of OK_BP, while the spherical model provided the best fit in the residuals of RK. At 30–50 cm, the spherical model provided the best fit to the semivariogram in OK and the residuals of RK, while the gaussian model provided the best fit in the residuals of OK_BP. The ranges and ratios of nugget/sill varied significantly. The values of the range varied from 429 m to 1000 m, which indicated that the grid spacing (240 m) was adequate for the characterization of the spatial variability. Cambardella et al. (1994) classified the strong, moderate and weak spatial dependency based on the ratios of nugget/sill at < 25%, 25%–75% and > 75%, respectively. For all the models, there was a moderately spatial correlation, which demonstrated that both intrinsic and extrinsic factors influenced soil electrical conductivity. Emadi and Baghernejad (2014) proved that compared with the weak

spatial correlation, the relatively strong spatial structure could create more accurate map.

3.5 Mapping spatial distribution of soil electrical conductivity

Fig. 4 revealed that the spatial distribution of soil electrical conductivity was similar by all four methods. The higher soil electrical conductivity was generally distributed in the west and southeast of the study area, and the lower soil electrical conductivity was mainly distributed in central area. According to the classification standards of soil salinization and the corresponding soil electrical conductivity in Ningxia (He et al., 2010; Wu et al., 2014), the non-salinized, slightly salinized, moderately salinized, severely salinized and saline-sodic soil were classified based on the soil electrical conductivity of < 0.34, 0.34–0.98, 0.98–1.87, 1.87–2.96, > 2.96 dS/m, respectively. Furthermore, if this accumulation reached 0.8 dS/m, salt toxicity occurred. At 0–30 cm soil depth, the central area was slightly salinized with soil electrical conductivity < 0.98 dS/m, which was mainly distributed in arable lands. The west and southeast area showed severely salinized to saline-sodic soil with soil electrical conductivity > 1.87 dS/m, specifically of > 2.96 dS/m, which were mainly distributed in the lower lying uncultivated land. At 30–50 cm depth, the soil in most areas was non-salinized to slightly salinized. In some localized areas, it was moderately salinized with soil electrical conductivity of more than 0.98 dS/m.

Table 4 Semivariogram parameters of soil electrical conductivity

Layer (cm)	Items	Model	Range (m)	Nugget	Partial sill	Nugget/sill (%)	R^2
0–30	Log (soil electrical conductivity)	Exponential	1000	0.715	1.325	35.05	0.643
	Log (Residuals _{RK})	Spherical	429	0.598	1.051	36.26	0.692
	Residuals _{OK_BP}	Exponential	911	0.979	1.417	40.86	0.792
30–50	Log (soil electrical conductivity)	Spherical	797	0.281	0.497	36.12	0.667
	Log (Residuals _{RK})	Spherical	430	0.106	0.176	37.59	0.757
	Residuals _{OK_BP}	Gaussian	863	0.705	1.095	39.17	0.829

Notes: Log (soil electrical conductivity) is log-transformed values of the raw soil electrical conductivity. Log (Residuals_{RK}) is log-transformed value of prediction residuals by multiple linear regression. Residuals_{OK_BP} is raw value of prediction residuals by ordinary kriging combined with back-propagation network.

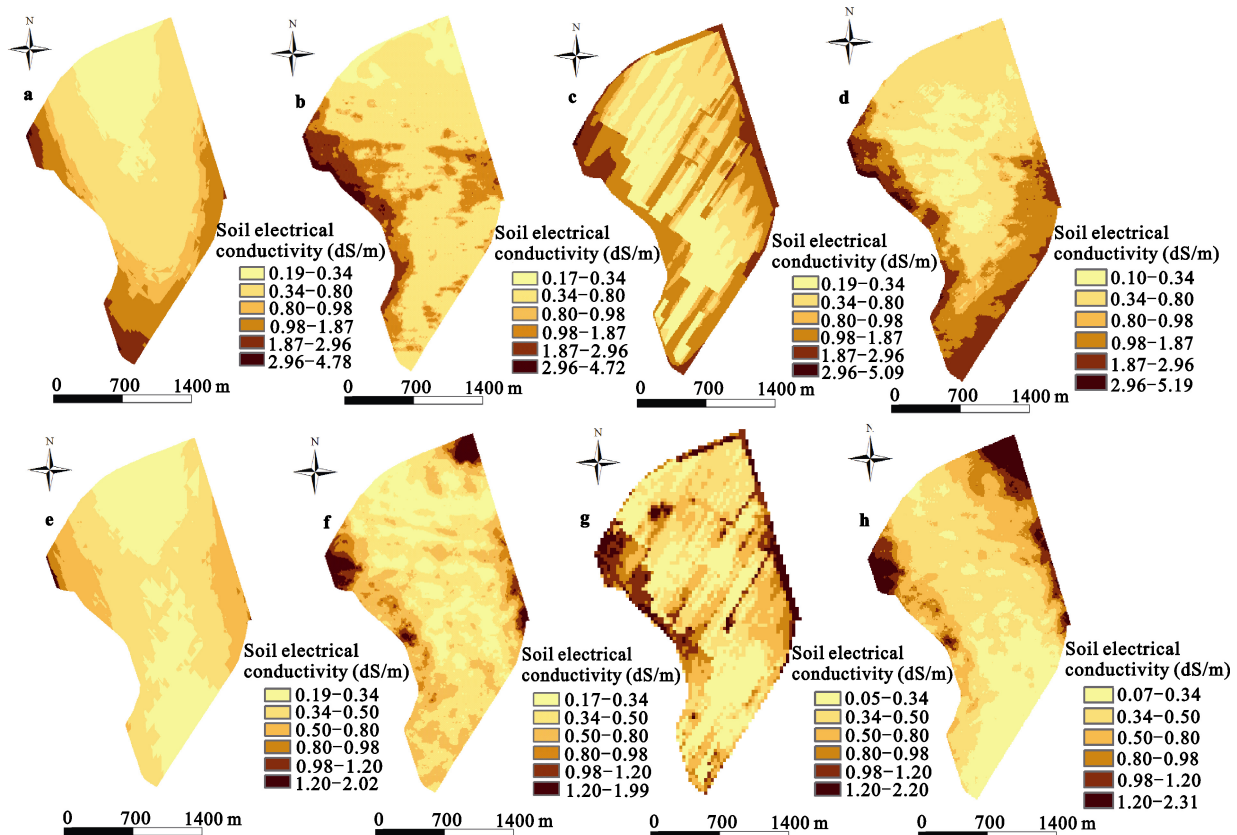


Fig. 4 Predicted spatial distribution of soil electrical conductivity (dS/m) using (a) ordinary kriging (OK), (b) back-propagation network (BP), (c) regression kriging (RK) and (d) ordinary kriging combined with back-propagation network (OK_BP) at 0–30 cm depth, and (e) ordinary kriging, (f) back-propagation network, (g) regression kriging and (h) ordinary kriging combined with back-propagation network at 30–50 cm depth

The differences between the mapping results were also obvious. At different soil depths, the mapping range of OK_BP was larger than that of other methods (i.e., RK, BP and OK). OK_BP effectively avoided underestimation of the higher values and overestimation of the lower values. The mapping polygons by OK_BP were relatively fragmentized, while the prediction maps by OK were smoother and integrated. Thus, OK_BP revealed more details of the spatial variation responding to the influencing factors. OK_BP provided more flexibility and capability for applying various influencing factors to the spatial prediction of soil properties. Furthermore, according to OK_BP mapping, it was obvious that the highest soil electrical conductivity was mainly distributed in the west part with the characteristic of the relatively lower terrain and NDVI, shorter distances from drainage ditches and uncultivated land distribution. Therefore, it can exhibit more realistic interpolation quality of OK_BP than that

of other methods.

3.6 Evaluating mapping accuracy of different methods

Table 5 showed the mapping accuracy of soil electrical conductivity at validation sites for the different methods. Considering the influencing factors as auxiliary information, the *MEs* of OK_BP were closer to 0 than those of other methods (i.e., OK, BP and RK) for mapping soil electrical conductivity. It suggested that OK_BP was a less biased model. OK_BP achieved the lowest *RMSE* of 0.340 dS/m and 0.171 dS/m at the two depths, respectively, which indicated a better agreement between the measured values with the predicted values than other mapping methods. Moreover, OK_BP achieved the highest *RI* and *DIP* among the four methods at the two depths, which suggested that the application of OK_BP could significantly improve the mapping accuracy of soil salinity at small scale.

Table 5 Mapping accuracy test of soil electrical conductivity

Layer (cm)	Method	<i>ME</i> (dS/m)	<i>RMSE</i> (dS/m)	<i>RI</i> (%)	<i>DIP</i> (%)
0–30	OK	−0.071	0.630	—	—
	BP	−0.079	0.562	10.794	37.576
	RK	−0.051	0.540	14.286	45.608
	OK_BP	−0.030	0.340	46.032	91.432
30–50	OK	−0.049	0.304	—	—
	BP	−0.032	0.278	8.553	28.227
	RK	−0.100	0.245	19.408	69.115
	OK_BP	−0.037	0.171	43.750	90.412

Notes: OK, ordinary kriging; BP, back-propagation network; RK, regression kriging; OK_BP, ordinary kriging combined with back-propagation network; *ME*, mean error; *RMSE*, root mean squared error; *RI*, relative improvement; *DIP*, decrease in the estimation imprecision.

4 Discussion

In this study, soil electrical conductivity at 0–30 cm soil depth is higher than that at 30–50 cm depth. This is due to the salt in the subsoil moving upward and accumulating in the topsoil as a result of evaporation (Jordán et al., 2004; Yu et al., 2014). This result is consistent with previous studies (Chi and Wang, 2010; Zhao et al., 2016), which find soil salinity surface accumulation. Soil electrical conductivity at 0–30 cm soil depth shows strong spatial variation (Table 1), and the mapping accuracies at 0–30 cm soil depth are lower than that of at 30–50 cm soil depth (Table 5). This can be attributable to the fact that topsoil salts are dynamic in nature, and complicated anthropogenic activities such as cultivation and irrigation may contribute significantly to spatial variation (Akramkhanov et al., 2011). Previous studies also emphasized that the surface soil properties were most modified by land management practices (Moore et al., 1993).

According to the sensitivity analysis, land use types, elevation, irrigation, drainage and NDVI are important factors influencing soil electrical conductivity. As shown in Table 2, land use types are the most sensitive to soil electrical conductivity. In another study (Nosetto et al., 2008; 2013), land use types is also found to be strongly sensitive to soil salinization. Land use is one of the most important anthropogenic causes of salinization, and has the potential to disrupt the water balance of a given territory and trigger salinization. Micro-topographic features, such as lower lying areas, are vulnerable to salinization. The lower topography together with the uncultivated land constrains surface drainage, whereas

high topography with the cultivated land employs drainage systems controlling salinization. Therefore, elevation variation may lead to different EC values, and is then determined sensitively. The distances from different sampling fields to the irrigation or drainage ditches present difference (Fig. 1). The irrigation networks and the existing drainage ditches are built to leach the soil salinity and lower the groundwater table respectively. The effects of the irrigation and drainage are directly reflected by changing the soil electrical conductivity (Akramkhanov et al., 2011). Therefore, irrigation and drainage are found to be moderately sensitive to soil salinity. NDVI is useful to determine the production of green vegetation, and lower NDVI values may correspond to high soil electrical conductivity due to low plantation stand (Aldakheel et al., 2011; Yahiaoui et al., 2015). However, uncultivated land with reeds and cultivated land with crop may present similar vegetation coverage in this study area. Thus, approximate NDVI values in study area may be less sensitive to soil salinity.

OK_BP is a hybrid model with more stable mapping performance and relatively higher mapping accuracy, which may be ascribed to the relationships between the soil properties and environmental factors that are rarely linear in nature (Zhao et al., 2010). First, on the basis of the relatively lower coefficient of determination (R^2) (Table 3), the MLR does not fully explain the complicated relationships. Meanwhile, the BP model has the ability of establishing nonlinear relationships through training directly. Accordingly, the BP is more appropriate than MLR to capture the relationships between the soil property and its influencing factors, which has been previously demonstrated (Zhao et al., 2010; Li et al., 2013; Shahabi et al., 2017). Second, OK_BP systematically

applies intrinsic and extrinsic factors to map soil electrical conductivity, and can capture both aspects of spatial variations caused by the local influencing factors and the spatial auto-correlation. Third, BP can deal with several issues, namely the reasonable change of scales (Akramkhanov and Vlek, 2012). Thus, OK_BP can effectively avoid underestimation of the higher values and overestimation of the lower values of the interpolation surface.

Before mapping soil salinity by OK_BP, the factors influencing soil electrical conductivity should be confirmed to be significant by sensitivity analysis or Pearson correlation coefficients. Factors such as climate, fertilization, groundwater table depth and groundwater quality may influence soil electrical conductivity at larger scales. In the future, further investigation of the incorporation of these factors into the OK_BP at larger scales is required. The auxiliary factors may further improve the performance of the model, but these are ongoing research topics beyond the scope of this study. Nevertheless, the results of this study indicate that OK_BP has the potential for modeling soil salinity and environmental characteristics.

5 Conclusions

In this study, sensitivity analysis shows that soil electrical conductivity is collectively influenced by the important orders of land use types, the distance to irrigation ditches, elevation, distance to drainage ditches and NDVI at 0–30 cm depth, and the important orders of land use types, elevation, distance to the irrigation ditches, distance to the drainage ditches and NDVI at 30–50 cm depth. Compared with other methods (i.e., OK, BP and RK), OK_BP systematically considers both aspects of spatial variations caused by influencing factors and its spatial autocorrelations. The mapping using OK_BP can generate more details of the spatial variation responding to the influencing factors, and effectively avoid underestimation of higher values and overestimation of lower values than other existing methods. Furthermore, OK_BP can improve the mapping accuracy of soil electrical conductivity, not only exhibiting the lowest *RMSE* of 0.340 dS/m and 0.171 dS/m among the four methods at the two depths, respectively, but also improving the accuracy of 46.032% and 43.750% compared with OK at the two depths, respectively. Thus, OK_BP is confirmed as an efficient way to understand soil salinization mechanism and improve the

mapping accuracy of soil salinity.

References

- Akramkhanov A, Martius C, Park S J et al., 2011. Environmental factors of spatial distribution of soil salinity on flat irrigated terrain. *Geoderma*, 163(1): 55–62. doi: 10.1016/j.geoderma.2011.04.001
- Akramkhanov A, Vlek P L G, 2012. The assessment of spatial distribution of soil salinity risk using neural network. *Environmental Monitoring and Assessment*, 184(4): 2475–2485. doi: 10.1007/s10661-011-2132-5
- Aldakheel Y Y, 2011. Assessing NDVI spatial Pattern as related to irrigation and soil salinity management in Al-Hassa Oasis, Saudi Arabia. *Journal of the Indian Society of Remote Sensing*, 39(2): 171–180. doi: 10.1007/s12524-010-0057-z
- Bilgili A V, 2013. Spatial assessment of soil salinity in the Harran Plain using multiple kriging techniques. *Environmental Monitoring and Assessment*, 185(1): 777–795. doi: 10.1007/s10661-012-2591-3
- Cambardella C A, Moorman T B, Parkin T B et al., 1994. Field-scale variability of soil properties in central low a soils. *Soil Science Society of America Journal*, 58(5): 1501–1511. doi: 10.2136/sssaj1994.03615995005800050033x
- Chen X H, Duan Z H, Luo T F, 2014. Changes in soil quality in the critical area of desertification surrounding the Ejina Oasis, Northern China. *Environmental Earth Sciences*, 72(7): 2643–2654. doi: 1007/s12665-014-3171-3
- Chi C M, Wang Z C, 2010. Characterizing salt-affected soils of Songnen Plain using saturated paste and 1:5 soil-to-water extraction methods. *Arid Land Research and Management*, 24(1): 1–11. doi: 10.1080/15324980903439362
- Dai F Q, Zhou Q G, Lv Z Q et al., 2014. Spatial prediction of soil organic matter content integrating artificial network and ordinary kriging in Tibetan Plateau. *Ecological Indicators*, 45: 184–194. doi: 10.1016/j.ecolind.2014.04.003
- Ding J L, Yu D L, 2014. Monitoring and evaluating spatial variability of soil salinity in dry and wet seasons in the Weri-gan-Kuqa Oasis, China, using remote sensing and electromagnetic induction instruments. *Geoderma*, 235: 316–322. doi: 10.1016/j.geoderma.2014.07.028
- Eldeiry A A, Garcia L A, 2012. Evaluating the performance of ordinary kriging in mapping soil salinity. *Journal of Irrigation and Drainage Engineering*, 138(12): 1046–1059. doi: 10.1061/(ASCE)IR.1943-4774.0000517
- Emadi M, Baghernejad M, 2014. Comparison of spatial interpolation techniques for mapping soil pH and salinity in agricultural coastal areas, northern Iran. *Archives of Agronomy and Soil Science*, 60(9): 1315–1327. doi: 10.1080/03650340.2014.880837
- Fang H L, Liu G H, Kearney M, 2005. Georelational analysis of soil type, soil salt content, landform, and land use in the Yellow River Delta, China. *Environmental Management*, 35(1): 72–83. doi: 10.1007/s00267-004-3066-2
- He B, Cai Y L, Ran W R et al., 2015. Spatiotemporal heterogene-

- ity of soil salinity after the establishment of vegetation on a coastal saline field. *Catena*, 127: 129–134. doi: 10.1016/j.catena.2014.12.028
- He Wenshou, Liu Yangchun, He Jinyu, 2010. Relationships between soluble salt content and electrical conductivity for different types of salt-affected soils in Ningxia. *Agricultural Research in the Arid Areas*, 28(1): 111–116. (in Chinese)
- Hengl T, Heuvelink G B M, Stein A, 2004. A generic framework for spatial prediction of soil variables based on regression-kriging. *Geoderma*, 120: 75–93. doi: 10.1016/j.geoderma.2003.08.018
- Huang Yajie, Ye Hechun, Zhang Shiwen et al., 2015. Zoning of arable land productivity based on self-organizing map in China. *Scientia Agricultura Sinica*, 48(6): 1136–1150. (in Chinese)
- Huang Y J, Ye H C, Zhang S W et al., 2017. Prediction of soil organic mMatter using ordinary kriging combined with the clustering of self-organizing map: a case study in Pinggu District, Beijing, China. *Soil Science*, 182: 52–62. doi: 10.1097/SS.0000000000000196
- Isaaks E H, Srivastava R M, 1989. *An Introduction to Applied Geostatistics*. New York: Oxford University Press.
- IUSS Working Group WRB, 2007. World reference base for soil resources 2006, first update 2007. *World Soil Resources Reports*, FAO, Rome. Available at: <http://www.fao.org>.
- Jordán M M, Navarro-Pedreno J, García-Sánchez E et al., 2004. Spatial dynamics of soil salinity under arid and semi-arid conditions: geological and environmental implications. *Environmental Geology*, 45(4): 448–456. doi: 10.1007/s00254-003-0894-y
- Lark R M, 1999. Soil-landform relationships at within-field scales: an investigation using continuous classification. *Geoderma*, 92(3–4): 141–165. doi: 10.1016/S0016-7061(99)00028-2
- Li Q Q, Yue T X, Wang C Q et al., 2013. Spatially distributed modeling of soil organic matter across China: an application of artificial neural network approach. *Catena*, 104: 210–218. doi: 10.1016/j.catena.2012.11.012
- Li Q Q, Zhang X, Wang C Q et al., 2016. Spatial prediction of soil nutrient in a hilly area using artificial neural network model combined with kriging. *Archives of Agronomy and Soil Science*, 62(11): 1541–1553. doi: 10.2136/sssaj1989.03615995005300030029x
- Liu T L, Juang K W, Lee D Y, 2006. Interpolating soil properties using kriging combined with categorical information of soil maps. *Soil Science Society of America Journal*, 70(4): 1200–1209. doi: 10.2136/sssaj2005.0126
- Lu Rukun, 2000. *Analysis methods of soil agricultural chemistry*. China: Agricultural Science and Technology Publishing House, 85–89. (in Chinese)
- McBratney A B, Santos M L M, Minasny B. 2003. On digital soil mapping. *Geoderma*, 117(1–2): 3–52. doi: 10.1016/S0016-7061(03)00223-4
- Mirakzehi K, Pahlavan-Rad M R, Shahriari A et al., 2018. Digital soil mapping of deltaic soils: a case of study from Hirmand (Helmand) river delta. *Geoderma*, 313: 233–240. doi: 10.1016/j.scitotenv.2018.02.052
- Mirlas V, 2012. Assessing soil salinity hazard in cultivated areas using MODFLOW model and GIS tools: a case study from the Jezre’el Valley, Israel. *Agricultural Water Management*, 109: 144–154. doi: 10.1016/j.agwat.2012.03.003
- Moore I D, Gessler P E, Nielsen G A et al., 1993. Soil attribute prediction using terrain analysis. *Soil Science Society of America Journal*, 57(2): 443–452. doi: 10.2136/sssaj1993.03615995005700020026x
- Mora-Vallejo A, Claessens L, Stoorvogel J et al., 2008. Small scale digital soil mapping in Southeastern Kenya. *Catena*, 76(1): 44–53. doi: 10.1016/j.catena.2008.09.008
- Motaghian H R, Mohammadi J, 2011. Spatial estimation of saturated hydraulic conductivity from terrain attributes using regression, kriging, and artificial neural networks. *Pedosphere*, 21(2): 170–177. doi: 10.1016/S1002-0160(11)60115-X
- Mozumder R A, Laskar A I, 2015. Prediction of unconfined compressive strength of geopolymer stabilized clayey soil using Artificial Neural Network. *Computers and Geotechnics*, 69: 291–300. doi: 10.1016/j.compgeo.2015.05.021
- Mueller T G, Mijatovic B, Sears B G et al., 2004. Soil electrical conductivity map quality. *Soil Science*, 169(12): 841–851. doi: 10.1097/00010694-200412000-00003
- Mueller T G, Pierce F J, 2003. Soil carbon maps: Enhancing spatial estimates with simple terrain attributes at multiple scales. *Soil Science Society of America Journal*, 67(1): 258–267. doi: 10.2136/sssaj2003.2580
- Nielsen D R, Bouma J, 1985. *Soil Spatial Variability: Proceedings of a Workshop of the ISSS and the SSSA, Las Vegas, USA /Pdc296*. Pudoc Wageningen, Netherlands: Center Agricultural Pub and Document.
- Nosetto M D, Acosta A M, Jayawickreme D H et al., 2013. Land-use and topography shape soil and groundwater salinity in central Argentina. *Agricultural Water Management*, 129: 120–129. doi: 10.1016/j.agwat.2013.07.017
- Nosetto M D, Jobbágy E G, Tóth T et al., 2008. Regional patterns and controls of ecosystem salinization with grassland afforestation along a rainfall gradient. *Global Biogeochemical Cycles*, 22(2): 1–12. doi: 10.1029/2007GB003000
- Olden J D, Jackson D A, 2002. Illuminating the ‘black box’: a randomization approach for understanding variable contributions in artificial neural networks. *Ecological Modelling*, 154(1–2): 135–50. doi: 10.1016/S0304-3800(02)00064-9
- Patel R M, Prasher S O, God P K, et al., 2002. Soil Salinity Prediction Using Artificial Neural Networks. *Journal of the American Water Resources Association*, 38(1): 91–100. doi: 10.1111/j.1752-688.2002.tb01537.x
- Park S J, Vlek P L G, 2002. Environmental correlation of three-dimensional soil spatial variability: a comparison of three adaptive techniques. *Geoderma*, 109(1–2): 117–140. doi: 10.1016/S0016-7061(02)00146-5
- Raczko E, Zagajewski B, 2017. Comparison of support vector machine, random forest and neural network classifiers for tree species classification on airborne hyperspectral APEX images. *European Journal of Remote Sensing*, 50(1): 144–154. doi:

- 10.1080/22797254.2017.1299557
- Sarangi A, Singh M, Bhattacharya A K et al., 2006. Subsurface drainage performance study using SALTMOD and ANN models. *Agricultural Water Management*, 84(3): 240–248. doi: 10.1016/j.agwat.2006.02.009
- Sedaghat A, Bayat H, Sinegani A A S, 2016. Estimation of soil saturated hydraulic conductivity by artificial neural networks ensemble in smectitic soils. *Eurasian Soil Science*, 49(3): 347–357. doi: 10.1134/S106422931603008X
- Shah S H H, Vervoort R W, Suweis S et al., 2011. Stochastic modeling of salt accumulation in the root zone due to capillary flux from brackish groundwater. *Water Resources Research*, 47(9): 09506–09522. doi: 10.1029/2010WR009790
- Shahabi M, Jafarzadeh A A, Neyshabouri M R et al., 2017. Spatial modeling of soil salinity using multiple linear regression, Ordinary kriging and artificial neural network methods. *Archives of Agronomy and Soil Science*, 63(2): 151–160. doi: 10.1080/03650340.2016.1193162
- Sheng J, Ma L, Jiang P et al., 2010. Digital soil mapping to enable classification of the salt-affected soils in desert agro-ecological zones. *Agricultural Water Management*, 97(12): 1944–51. doi: 10.1016/j.agwat.2009.04.011
- Taghizadeh-Mehrjardi R, Ayoubi S, Namazi Z et al., 2016. Prediction of soil surface salinity in arid region of central Iran using auxiliary variables and genetic programming. *Arid Land Research and Management*, 30(1): 49–64. doi: 10.1080/15324982.2015.1046092
- Takata Y, Funakawa S, Akshalov K et al., 2007. Spatial prediction of soil organic matter in northern Kazakhstan based on topographic and vegetation information. *Soil Science and Plant Nutrition*, 53(3): 289–299. doi: 10.1111/j.1747-0765.2007.00142.x
- Visconti F, de Paz J M, Rubio J L, 2010. What information does the electrical conductivity of soil water extracts of 1 to 5 ratio (w/v) provide for soil salinity assessment of agricultural irrigated lands? *Geoderma*, 154 (3–4): 387–397. doi: 10.1016/j.geoderma.2009.11.012
- Wang S Q, Song X F, Wang Q X et al., 2012. Shallow groundwater dynamics and origin of salinity at two sites in salinated and water-deficient region of North China Plain, China. *Environmental Earth Sciences*, 66(3): 729–739. doi: 10.1007/s12665-011-1280-9
- Wang S, Adhikari K, Wang Q B et al., 2018. Role of environmental variables in the spatial distribution of soil carbon (C), nitrogen (N), and C: N ratio from the northeastern coastal agroecosystems in China. *Ecological Indicators*, 84: 263–272. doi: 10.1016/j.ecolind.2017.08.046
- Were K, Bui D T, Dick Ø B et al., 2015. A comparative assessment of support vector regression, artificial neural networks, and random forests for predicting and mapping soil organic carbon stocks across an Afromontane landscape. *Ecological Indicators*, 52: 394–403. doi: 10.1016/j.ecolind.2014.12.028
- Wu J H, Li P Y, Qian H et al., 2014. Assessment of soil salinization based on a low-cost method and its influencing factors in a semi-arid agricultural area, northwest China. *Environmental Earth Sciences*, 71(8): 3465–3475. doi: 10.1007/s12665-013-2736-x
- Yahiaoui I, Douaoui A, Zhang Q et al., 2015. Soil salinity prediction in the Lower Chelif plain (Algeria) based on remote sensing and topographic feature analysis. *Journal of Arid Land*, 7(6): 794–805. doi: 10.1007/s40333-015-0053-9
- Yang Q Y, Jiang Z C, Li W J et al., 2014. Prediction of soil organic matter in peak-cluster depression region using kriging and terrain indices. *Soil and Tillage Research*, 144: 126–132. doi: 10.1016/j.still.2014.07.011
- Ye H C, Huang W J, Huang S Y et al., 2017. Effects of different sampling densities on geographically weighted regression kriging for predicting soil organic carbon. *Spatial Statistics*, 20: 76–91. doi: 10.1016/j.jspasta.2017.02.001
- Ye H C, Huang Y F, Chen P F et al., 2016. Effects of land use change on the spatiotemporal variability of soil organic carbon in an urban–rural ecotone of Beijing. *Journal of Integrative Agriculture*, 15(4): 918–928. doi: 10.1016/S2095-3119(15) 61066-8
- Yu J B, Li Y Z, Han G X et al., 2014. The spatial distribution characteristics of soil salinity in coastal zone of the Yellow River Delta. *Environmental Earth Sciences*, 72(2): 589–599. doi: 10.1007/s12665-013-2980-0
- Yu S H, Liu J T, Eneji A E et al., 2015. Spatial Variability of Soil Salinity under Subsurface Drainage. *Communications in Soil Science and Plant Analysis*, 46(2): 259–270. doi: 10.1080/00103624.2014.967863
- Zhang F, Tiyip T, Ding J L et al., 2009. The effects of the chemical components of soil salinity on electrical conductivity in the region of the Delta Oasis of Weigan and Kuqa Rivers. *Agricultural Sciences in China*, 8(8): 985–993. doi: 10.1016/S1671-2927(08)60304-1
- Zhang S W, Huang Y F, Shen C Y et al., 2012. Spatial prediction of soil organic matter using terrain indices and categorical variables as auxiliary information. *Geoderma*, 171: 35–43. doi: 10.1016/j.geoderma.2011.07.012
- Zhang S W, Shen C Y, Chen X Y et al., 2013. Spatial interpolation of soil texture using compositional kriging and regression kriging with consideration of the characteristics of compositional data and environment variables. *Journal of Integrative Agriculture*, 12(9): 1673–1683. doi: 10.1016/S2095-3119(13) 60395-0
- Zhao Y, Feng Q, Yang H D, 2016. Soil salinity distribution and its relationship with soil particle size in the lower reaches of Heihe River, Northwestern China. *Environmental Earth Sciences*, 75(9): 1–18. doi: 10.1007/s12665-016-5603-8
- Zhao Z Y, Yang Q, Benoy G et al., 2010. Using artificial neural network models to produce soil organic carbon content distribution maps across landscapes. *Canadian Journal of Soil Science*, 90(1): 75–87. doi: 10.4141/CJSS08057
- Zhu A X, 2000. Mapping soil landscape as spatial continua: the neural network approach. *Water Resources Research*, 36(3): 663–677. doi: 10.1016/S1671-2927(08)60349-1
- Zou P, Yang J S, Fu J R et al., 2010. Artificial neural network and time series models for predicting soil salt and water content. *Agricultural Water Management*, 97(12): 2009–2019. doi: 10.1016/j.agwat.2010.02.011